

Ultraviolet Spectroscopy Experiment for Mariner Mars 1971¹

C. W. HORD, C. A. BARTH, AND J. B. PEARCE

Laboratory for Atmospheric and Space Physics, University of Colorado, Boulder, Colorado 80302

Received March 24, 1969; Revised August 4, 1969

The Mariner Mars 1971 ultraviolet spectrometer will obtain spectra in the 1100 to 3400 Å wavelength range. The spectral features in this range will help to characterize the Martian atmosphere in a quantitative way. At wavelengths near 3400 Å, the spectra may be dominated by ground reflection because of the low surface pressure on Mars.

Spectra from the outermost part of the Martian atmosphere will be dominated by resonance scattering of solar radiation by atomic species such as hydrogen, oxygen, and nitrogen. Somewhat lower down in the atmosphere, major atmospheric species can be observed. Solar radiation can excite molecular species through resonance reradiation, fluorescence, and photoelectron excitation. Many of these possible neutral and ionic constituents, such as carbon monoxide, molecular nitrogen, and ionized carbon dioxide, reradiate in the ultraviolet. The spectra from the lower Martian atmosphere, i.e., within a scale height or so of the planet surface, will be dominated by absorption below 2000 Å. The dominant signal longward of 2000 Å will be due to Rayleigh scattering by carbon dioxide, and Mie scattering from clouds. If a loosely bound molecular species such as ozone is present, then a broad absorption feature can appear in the 2000 to 3000 Å wavelength region.

The atmospheric composition of Mars may be indicative of biological activity. In this sense, ultraviolet spectroscopy will contribute to a biological understanding of the planet.

I. INTRODUCTION

Scientific objectives of the ultraviolet spectroscopy experiment for the Mariner Mars 1971 orbital missions are divided into two categories: (1) ultraviolet cartography, the mapping of the surface and lower atmosphere in the ultraviolet spectral region; and (2) ultraviolet aeronomy, the study of the composition and structure of the upper atmosphere using the techniques of ultraviolet spectroscopy. The ultraviolet

cartography measurements will be accomplished by pointing the spectrometer at the illuminated disk of Mars. The upper atmospheric measurements require the use of different geometries in order to view the upper atmosphere and to discriminate against the bright, lower atmosphere of Mars.

The specific objectives included in ultraviolet cartography are (1) to measure local atmospheric pressure over a major part of the planet, (2) to measure local ozone concentration, and (3) to measure the Mars photometric function in the near-ultraviolet. Ultraviolet spectra of phenomena associated with Mars, such as the wave of darkening, white and yellow clouds, and the blue haze-blue clearing phenomenon, are included in this category. Implicit in

¹ This work was performed for the Jet Propulsion Laboratory, California Institute of Technology, sponsored by the National Aeronautics and Space Administration, under Contract No. NAS 7-100; this work was also supported by the National Aeronautics and Space Administration, under research grant NGL 06-003-052.

the ozone measurements is the search for evidence of biological activity that might occur in suitable microenvironments on Mars.

The specific objectives included in ultraviolet aeronomy are (1) to measure composition and structure of the upper atmosphere as a function of latitude, longitude, and time; (2) to measure ionosphere composition and its variations; and (3) to measure distribution and escape rate of atomic hydrogen from the exosphere. The distribution and variability of possible ultraviolet aurora, which might be indicative of an induced planetary magnetic field, will be explored.

II. ULTRAVIOLET CARTOGRAPHY

At wavelengths greater than about 2000 Å, a large part of the solar radiation will penetrate deep into the Martian atmosphere; in fact, much of this radiation may reach the planet's surface. In discussing ultraviolet cartography, we will be concerned with the ultraviolet spectra in the 2000 to 3400 Å wavelength interval. When viewing the illuminated disk in this wavelength range, the ultraviolet spectrometer will provide a spectrometric map of the planet. A similar ultraviolet spectroscopy experiment, on the OGO-4 satellite, has been orbiting the Earth since July 1967 (Barth and Mackey, 1969). What is an upper atmosphere experiment on the Earth, however, becomes a lower atmosphere experiment on Mars, where the surface pressure corresponds to the 30 to 35 km level on Earth.

The tenuous nature of the Martian atmosphere makes possible some unique ultraviolet measurements that would not be possible on the Earth or Venus. The S-band occultation experiment on the Mariner flyby mission in 1964 indicated that the surface pressure on Mars is about 6 mb or roughly 1/170 of the surface pressure on the Earth (Kliore, Cain, and Levy, 1967). With this pressure, and a nominal surface temperature of 200°K, the number density of the atmosphere at the surface of the planet would be about 2×10^{17} molecules/cm³. If one assumes

carbon dioxide to be the major atmospheric constituent near the planet's surface, then the atmospheric scale height would be about 10 km. The number of molecules in a vertical column above the surface will be 2×10^{23} molecules/cm² column. If one calculates the optical thickness, τ , of such a tenuous atmosphere, with Rayleigh scattering assumed to be the primary extinction mechanism, the resulting optical depths are quite small. At 2000 Å, $\tau = 0.17$, and τ is still smaller as the wavelength increases toward the visible part of the spectrum. The implication of such a small optical depth is that a large fraction of the solar flux πF (2000 to 3400 Å) reaches the Martian surface. The existence of sizable amounts of gases such as molecular nitrogen would not alter this picture appreciably, as they are all relatively transparent in the 2000 to 3400 Å range. If radiation at middle ultraviolet wavelengths does not reach the ground (or a boundary layer close to the ground), then one must postulate the existence of a loosely bound molecular species such as ozone, which absorbs strongly at these wavelengths. An alternate explanation would be that clouds of sufficient opacity exist to prevent penetration of this radiation to the planet's surface.

1. Surface Pressure

If the dominant opacity of the Martian atmosphere in the ultraviolet is indeed governed by Rayleigh scattering, then the local surface pressure can be measured (Sagan, and Pollack, 1966; 1968; Pollack, 1967). If one assumes that the planet's surface is a very efficient absorber in the ultraviolet, having an albedo as small as 0.04, then the ultraviolet spectrometer would view the atmospheric gas against a nearly black background (Evans, 1965). As the atmosphere is optically thin, the apparent emission rate, $4\pi\mathcal{A}$, is proportional to N , the number of molecules/cm² column along the line of sight of the ultraviolet spectrometer. In this discussion, it is assumed that all of the molecules in the instrument's field of view are illuminated by the Sun. Under these

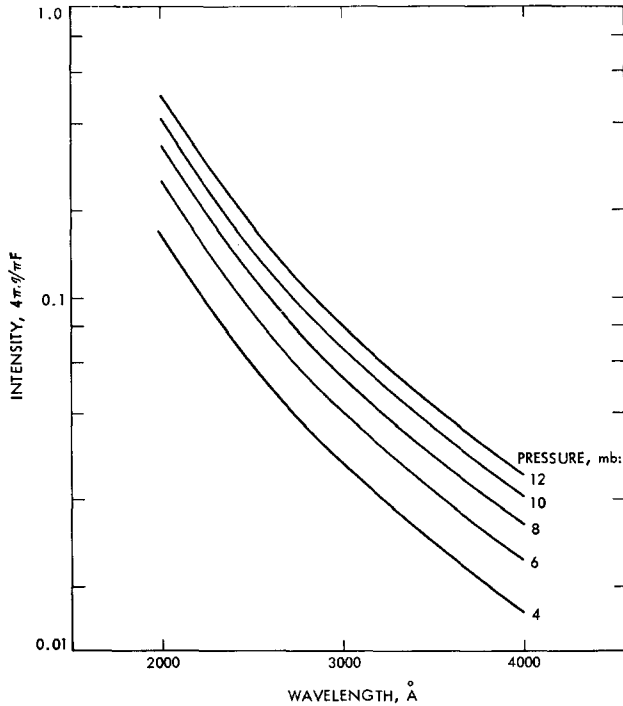


FIG. 1. Intensity variation due to surface pressure.

conditions, the intensity is related to the column density by the equation

$$4\pi\mathcal{A}(\lambda) = \pi F(\lambda) \frac{3}{4}(1 + \cos^2 \phi) \sigma_R(\lambda) N, \quad (1)$$

where $\pi F(\lambda)$ is the solar flux at Mars, $\sigma_R(\lambda)$ is the Rayleigh scattering cross section, N is the column density, and ϕ is the scattering angle. As the solar flux is known (Tousey, 1963) and the Rayleigh cross sections of carbon dioxide and other gases such as molecular nitrogen that might be present in significant amounts are also known, one can infer column densities from ultraviolet spectrometer intensity measurements. Knowledge of N then relates to the surface pressure by the equations

$$N = nH$$

$$H = \frac{kT}{Mg}$$

and

$$p = nkT$$

so that

$$N = \frac{p}{Mg}$$

and

$$4\pi\mathcal{A}(\lambda) = \pi F(\lambda) \frac{3}{4}(1 + \cos^2 \phi) \sigma_R(\lambda) \frac{p}{Mg}, \quad (2)$$

where n is the number density at the planet's surface, H is the scale height of the lower atmosphere, p is the surface pressure, T is the surface temperature, k is Boltzmann's constant, M is the mean molecular weight of the atmospheric gas, and g is the acceleration due to gravity. The significant fact is that $4\pi\mathcal{A}$ is proportional to the pressure at the surface of Mars. If, for example, the scale height is 10 km near the surface of Mars, then a 1-km change in average elevation of the Martian surface averaged over the ultraviolet spectrometer field of view would translate into a 10% intensity variation, as detected by the ultraviolet spectrometer. This is true, since the surface pressure variation with altitude is

$$p(z) = p(0) \exp(-z/h),$$

where $p(0)$ is the pressure at the reference altitude, $z = 0$. Measurements of this type

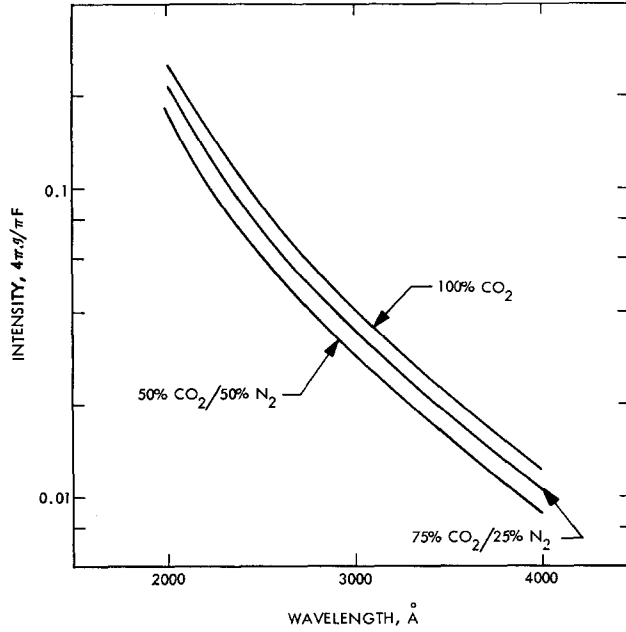


Fig. 2. Intensity variation due to atmospheric composition.

will be particularly useful when coupled with the local atmospheric temperature provided by infrared measurements and the results of the occultation experiments.

If there are wavelengths in the ultraviolet where atmospheric Rayleigh scattering is the dominant process, relative to ground reflectivity and atmospheric absorption,

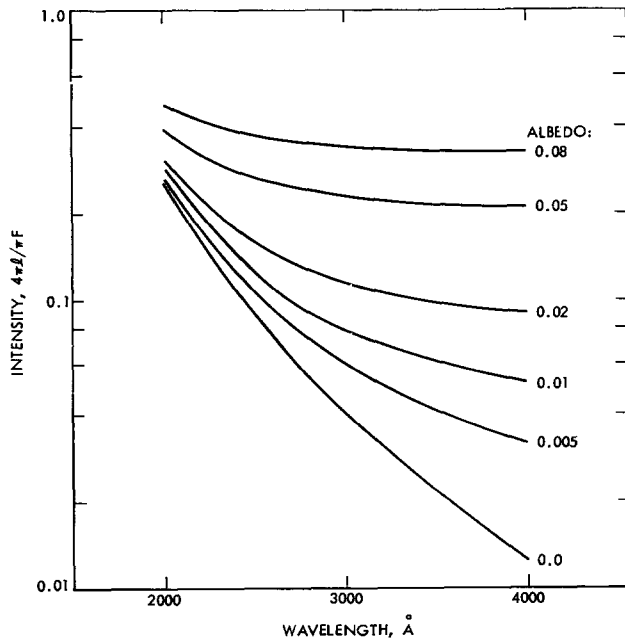


Fig. 3. Intensity variation due to surface albedo.

then the Mariner Mars 1971 orbiter will provide the opportunity to map the local atmospheric pressure. Figures 1 and 2 show how the ultraviolet intensity (measured in units of the solar flux) varies with wavelength for different surface pressures and for different mixtures of carbon dioxide and molecular nitrogen. In these figures, it has been assumed that the planet's surface provides a black background.

2. Surface Albedo

Mars may have a nonnegligible surface albedo, $A(\lambda)$, particularly in the longer part of the wavelength range. Figure 3 shows the effect of small values of A . In Fig. 3, A is taken to be independent of wavelength. It is seen that the effect of an albedo as large as 0.05 dominates the reflected spectrum, especially at longer wavelengths. In fact, albedos less than 0.005 are clearly measurable at the longer wavelength part of the ultraviolet range. It is seen that at shorter wavelengths Rayleigh scattering is still dominant, meaning that surface pressure measurements are possible at the shorter wavelengths. Variations in the surface character may be mapped out if there are wavelengths that reach the ground. This will be particularly valuable information when coupled with the knowledge of the visual wavelength albedo over the surface and the infrared spectrometer measurements.

3. Clouds and Haze

Another possibility is that clouds could be opaque enough to prevent ultraviolet radiation from reaching the Martian surface. In this case, the spectrometer would sample, by Rayleigh scattering, the atmosphere above the ultraviolet cloudtops. In addition, the Mie-scattered radiation from the clouds may provide some information about the cloud particles. The wavelength dependence of Mie scattering is significantly different from Rayleigh scattering, at least for larger particles, so the separation of these effects may be possible. The molecular scattering part of the signal would provide pressure measurements at the ultraviolet cloudtops. This information coupled with the scale height

would provide altitude information about the clouds. Variation in cloud cover with time and planet locality would be detectable if the cloud size were larger than, or comparable to, the 10-km² field of view.

It has been suggested that the Mars polarimetry data indicate the presence of a planet-wide haze of Mie-scattering aerosols (Rea and O'Leary, 1965). If a significant haze does exist, then ultraviolet spectra on both sides of the terminator should show its existence. The intensity contribution from the planet's surface disappears as the terminator is crossed, and the remaining signal will then have a wavelength dependence indicative of the scatterer. If the interpretation of the Martian photometry and polarimetry measurements by Pollack and Sagan (1967) is correct, then the scattering from the planet's surface is lost upon crossing the terminator, and the remaining intensity will be due to Rayleigh scattering, $1/\lambda^4$, from the atmospheric species. If Mie scattering by a planet-wide haze is an important factor, then the wavelength dependence of the intensity after crossing the terminator will be indicative of Mie scattering, $\sim 1/\lambda$.

4. Ozone

Ozone may be measured in a planetary atmosphere by means of the absorption of ultraviolet light between 2000 and 3000 Å due to the Hartley band system. The intensity of light scattered by an atmosphere undergoing both Rayleigh scattering and ozone absorption is given by the following equation:

$$4\pi\mathcal{A}(\lambda) = \frac{\pi F(\lambda)}{\mu} \frac{3}{4} (1 + \cos^2 \phi) \int_0^\infty \sigma_R(\lambda) n_R \times \exp \left[- \left(\int_z^\infty \frac{1}{\mu_0} + \frac{1}{\mu} \right) \sigma_{O_3}(\lambda) n_{O_3} dz' \right] dz, \quad (3)$$

where σ_R and σ_{O_3} are the Rayleigh scattering and ozone absorption coefficients, respectively. The number densities of ozone and the Rayleigh scattering constituent are n_{O_3} and n_R , respectively. The cosine of the solar zenith angle is μ_0 and the cosine of the emission angle is μ . The

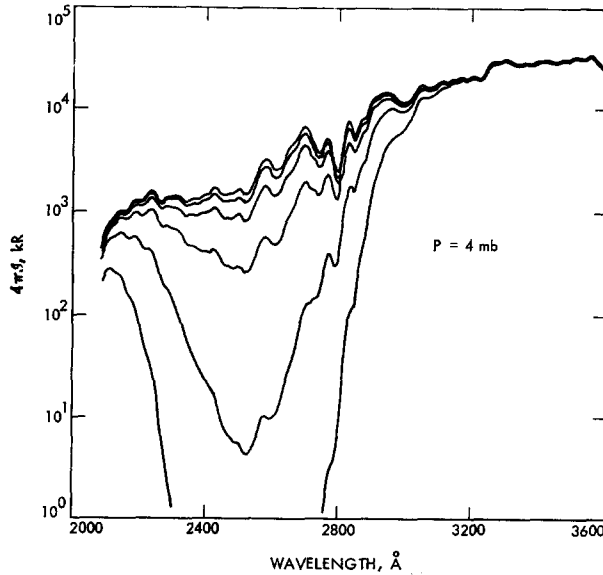


FIG. 4. Synthetic spectrum of illuminated disk of Mars assuming varying amounts of ozone: 0.0003, 0.001, 0.003, 0.01, 0.3 cm-atm. The ground (Bond) albedo is taken to be constant and equal to 0.04. The Rayleigh scattering constituent is assumed to be CO_2 . An apparent emission rate, $4\pi\mathcal{A} = 1 \text{ kR}$, corresponds to a brightness, $\mathcal{A} = 10^9/4\pi \text{ photons cm}^{-2} \text{ sec}^{-1} (20 \text{ \AA})^{-1}$.

inversion of this equation gives the ozone distribution as a function of height. Observations of the Earth in this spectral region have been made by the ultraviolet spectrometer on the OGO-4 satellite (Barth and Mackey, 1969). Anderson *et al.* (1969) have inverted Eq. (3) to obtain an ozone distribution using the OGO-4 ultraviolet spectrometer data. There are detailed variations in the spectrum due to Fraunhofer lines in the solar spectrum, while a large dip occurs between 2000 and 3000 Å with a maximum at 2500 Å due to ozone absorption. The amount of ozone in the Earth's atmosphere is equivalent to a thickness of 0.3 cm at standard temperature and pressure. In Figs. 4, 5, and 6, the expected intensity appropriate to Mars is plotted for varying amounts of ozone, 0.0003, 0.001, 0.003, 0.01, 0.03 cm, all much less than the amount on Earth. The surface albedo is taken to be 0.04, and the assumed surface pressures are 4, 9, and 20 mb. The measurement of ozone by this technique is a sensitive method of detecting the presence of molecular oxygen in a planetary atmosphere; the formation of ozone is preceded by the photodissociation

of molecular oxygen to form oxygen atoms. The oxygen atoms react with other oxygen molecules to form ozone. The ozone is destroyed by photodissociation and reactions with atomic oxygen. The equilibrium density of ozone is a function of the amount of molecular oxygen present; conversely, the amount of molecular oxygen may be inferred from a measurement of the amount of ozone.

Through the ultraviolet spectroscopy experiment, amounts of ozone equivalent to a molecular oxygen concentration of biological significance, 0.1% (Barth, 1969), can be detected. Belton and Hunten (1968) suggest that the upper limits previously placed on the amount of molecular oxygen in the Martian atmosphere may be too low, and they discuss a possible detection of oxygen in the Martian atmosphere.

The ultraviolet spectrometer (F-channel) will have a projected field of view of approximately $10 \times 10 \text{ km}$ on the ground at the periapsis altitude of 1600 km. This high spatial resolution will make it possible to search for microenvironments that have ozone and to determine whether localities of enhanced ozone concentration occur on

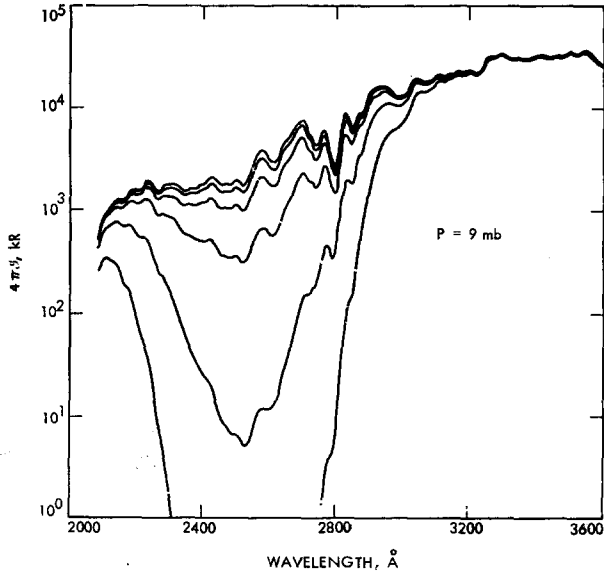


FIG. 5. Synthetic spectrum of illuminated disk of Mars assuming varying amounts of ozone: 0.0003, 0.001, 0.003, 0.01, 0.03 cm-atm.

Mars. The greater pressure in the low-lying regions may cause the ozone density to be larger. The ozone may be in contact with the surface and react with different surface materials. The oxidized state of the surface may, in fact, be due to ozone. Different surface materials may react in

varying degrees with ozone, producing local variations in the ozone concentration and in the characteristics of the surface. There may be local areas where biological activity may produce molecular oxygen. Photodissociation in turn will lead to the formation of ozone. The ozone then could

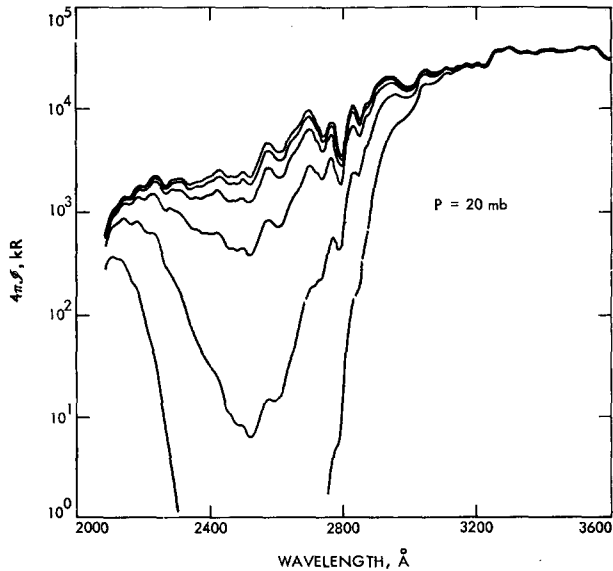


FIG. 6. Synthetic spectrum of Mars illuminated disk assuming varying amounts of ozone: 0.0003, 0.001, 0.003, 0.01, 0.03 cm-atm.

protect the bottom of the craters from ultraviolet radiation and permit greater biological activity. The measurement of ozone abundances in localized areas in amounts that exceed what may be explained by physical processes may be interpreted as indicative of biological activity.

Variable ozone production may be involved in the wave of darkening, whether or not that phenomenon is due to a physical or a biological process. The wave of darkening is a seasonal phenomenon that may be related to the amount of solar radiation reaching the surface of the planet. Ozone formation is also regulated by the intensity of the solar radiation. It should be determined whether the two phenomena are interrelated. The interaction between the wave of darkening and the ozone concentration may be an oxidation of the surface, or a shielding of biological activity on the surface from ultraviolet radiation. It is possible that another loosely bound molecular absorber, such as nitrogen dioxide, absorbs in the middle ultraviolet on Mars. The absorption features of middle-ultraviolet absorbers are broad, but have different variations with wavelength and are distinguishable at 20-Å resolution.

Let us summarize the results that might be expected from spectral scans covering the wavelength interval from 2000 to 3400 Å with the instrument pointed at the illuminated disk of Mars. In this wavelength range, the reflectivity of Mars will be dominated by four physical phenomena: (1) reflectivity of the surface, (2) Rayleigh scattering by the atmosphere, (3) absorption by atmospheric constituents such as ozone, if present, and (4) Mie scattering by clouds or haze, if present. Each of these phenomena has a different dependence on wavelength. Spectral scans covering the wavelength range between 2000 and 3400 Å should make it possible to separate these four effects, especially when taken under different viewing conditions and above regions with different surface reflectivities. Our present knowledge of Mars would lead us to expect that Rayleigh scattering would be the dominant process at the shorter wavelength end of the spectrometer range;

the middle-wavelength range would be dominated by ozone; at longer wavelengths, the reflection characteristics of the Martian surface would dominate. The pressure, as determined by the spectrometer measurements, will also be correlated with the pressure measurements made by the S-band occultation experiment. Both measurements are based on the same fundamental molecular property, i.e., the electric polarizability of the atmospheric molecules. In addition, the infrared spectroscopy experiment will provide measurements of the pressure near the surface by observing the pressure broadening of CO₂ absorption features.

III. ULTRAVIOLET AERONOMY

Observations of the photoelectron-excited and resonance-scattering ultraviolet dayglow between 1100 and 1900 Å provide a method of measuring the distribution of the major constituents in the upper atmosphere of Mars. The photoelectrons that result from the ionization of the atmosphere by solar extreme ultraviolet radiation excite the atoms and molecules that are the major constituents in the thermosphere. The photoelectron excitation mechanism in the Earth's atmosphere has been discussed by Green and Barth (1967) and Dalgarno, McElroy, and Stewart (1969). Examples of the dayglow emissions in the 1100 to 1900 Å range are shown by Barth (1969). Atomic lines from hydrogen (1216 Å), oxygen (1304 Å), nitrogen (1200 Å), and carbon (1657 Å) occur in this wavelength range. The fourth positive bands of carbon monoxide and the Lyman-Birge-Hopfield bands of molecular nitrogen are produced by photoelectron excitation. The actual intensity ratio between emissions from different atoms and molecules depends, of course, on their relative abundance in the atmosphere and the cross section for the particular emission. The height at which the maximum emission from the photoelectron-excited dayglow occurs is determined by the depth of penetration of the ionizing radiation. The measurement of the dayglow as a function of solar zenith angle is a way of determining the

height distribution of the major atmospheric constituents. In the thermosphere, where diffusive equilibrium exists, the lighter atoms rise above the heavier molecules. A complete global map of the photoelectron-excited dayglow, such as will be obtained from many successive orbits, will show variations in the atmospheric structure as a function of time. For example, changes in the amount of solar heating will affect the structure by changing the scale height for diffusive equilibrium.

Other molecular band systems undergo fluorescent scattering, which can be measured as part of the twilight glow. The γ -bands of nitric oxide and the Cameron bands of carbon monoxide appear in fluorescence. Measurement of these twilight emissions can give the distribution of these molecules as a function of height at the terminator. Repeated twilight measurements can show changes in the structure of the atmosphere as a function of latitude and of time. Minor constituents such as nitric oxide may be used to indicate what atmospheric motions are occurring.

The most likely ions in the Martian ionosphere are CO_2^+ and CO^+ . These molecular ions have fluorescent spectra in the 2100 to 2900 Å region. Barth (1969) gives synthetic spectra of the first negative bands of CO^+ and the emission bands of CO_2^+ . These ions and their distribution with height may be measured at twilight. When these results are combined with radio occultation measurements taken at different times from the orbiter, the structure of the ionosphere may be determined as a function of time. Repeated twilight passes occurring at different latitudes would permit also a measurement of changes along the terminator.

The synthetic spectra of a number of the band systems discussed here as well as the associated emission rate factors are given by Barth (1969). The emission rate factors, in effect, specify the sensitivity of the spectrometer to the various species.

Atomic hydrogen produces an ultraviolet dayglow line at 1216 Å by the resonance scattering of solar radiation. The intensity of this emission is a measure

of the density of atomic hydrogen (Thomas, 1963). The temperature may be determined from the variation of the intensity as a function of planetocentric distance (Barth, Wallace, and Pearce, 1968). The escape rate of atomic hydrogen may be determined from a knowledge of the density and temperature. On Mars, where the gravitational attraction is much less than on Earth, the escape rate is greater. The escape rate may vary on a time scale measured in days, either because of an increase in the temperature of the upper atmosphere due to solar activity or because of a change in the supply of atomic hydrogen to the upper atmosphere. Such a change might come about, for example, if water vapor is released into the atmosphere during the melting of the ice caps. The change in escape rate, as measured by a change in the density of atomic hydrogen, could take place during a Martian season.

Ultraviolet aurora are observed on both the night and day sides of the Earth by the ultraviolet spectrometer on the OGO-4 satellite. It is possible that aurora may also be observed on Mars. The following physical processes could lead to an aurora on Mars. When the solar wind interacts with a conducting atmosphere, an induced magnetic field is produced. This induced field, in turn, guides the charged particles of the solar wind around the planet and perhaps into the atmosphere. The energy carried by the protons is transferred to the electrons, which then interact with the atmosphere. Such an effect would be symmetric with the subsolar point and produce an auroral ring near the terminator on either the night or day side. The ultraviolet spectrometer can distinguish ultraviolet emissions from charged-particle bombardment and can give information about a possible auroral region on Mars.

IV. MEASUREMENT GEOMETRY

Four fundamental measurement geometries for the ultraviolet spectrometer are shown in Fig. 7 and are identified as the (1) bright limb, (2) illuminated disk, (3) terminator, and (4) dark limb. The

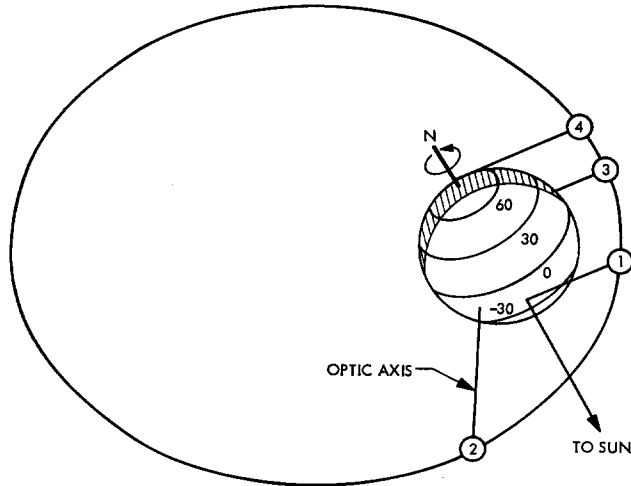


Fig. 7. Four fundamental geometries to be used by the ultraviolet spectrometer.

Lyman- α resonance line of atomic hydrogen can be observed in all of these geometries and, in fact, would be seen throughout an orbit. The Earth's Lyman- α radiation can be observed out to 100,000 km and on Venus to 20,000 km (Barth *et al.*, 1967).

For wavelengths below 2000 Å, the CO₂ lower atmosphere absorbs efficiently and provides a black background against which the emission features of the upper atmosphere stand out. The solar excited features differ in intensity for the bright limb, illuminated disk, and the terminator cases, primarily because of geometry differences. In the case of optically thick lines and bands, multiple scattering will modify the observed intensities.

Longward of 2000 Å, the lower atmosphere no longer served as a black background for upper atmospheric spectral features, and the geometry differences are more important. When observing the illuminated disk, one could expect the signal to be dominated by Rayleigh scattering from CO₂ because there is so much of it; the ozone-Hartley band absorption, because the cross section, $\sigma = 10^{-17}$ cm², is so large; and by ground reflection, because a large fraction of the radiation reaches the ground. In addition, Mie scattering from clouds may be important. The intensities expected are about four orders of magnitude larger than the

emissions from the upper atmospheric constituents in this wavelength region. The bright limb and terminator geometries provide discrimination against the bright lower atmosphere for wavelengths in the 2000 to 3400 Å range. In the case of the terminator geometry, this discrimination occurs because the lower atmosphere is not directly illuminated by solar radiation. The bright-limb geometry depends upon effective discrimination against off-axis light.

1. Bright Limb

Let us consider the bright-limb geometry in some detail. First, the response function of the spectrometer must fall off rapidly outside of the central field of view to allow for effective off-axis light discrimination. The Mariner instrument has an effective baffling arrangement that reduces the sensitivity of the instrument by more than a factor of 10⁵ at 1 deg off-axis. The Mariner Mars ultraviolet spectrometer slit function falls off exponentially with off-axis angle, for angles more than a degree outside the central field of view. In cases where the off-axis response has axial symmetry, the intensity can be written

$$4\pi\mathcal{A}(\text{off-axis}) = 4\pi\mathcal{A}(\text{disk})\rho(\theta_0) \times \frac{\pi\theta_H^2}{\Omega_0} f\left(\frac{\theta_0}{\theta_H}\right), \quad (4)$$

where $4\pi\mathcal{A}$ (disk) is the brightness of the planet disk, taken to be constant. The point source response function for an angle θ_0 between the planet limb and optic axis is $\rho(\theta_0)$, where $\rho(\theta)$ is normalized so that $\rho(0) = 1$. The scale factor for the off-axis response function is θ_H ; Ω_0 is the solid angle of the central field of view

$$\Omega_0 \equiv \int \rho(\theta) d\Omega \quad (5)$$

and $f(\theta_0/\theta_H)$ is a factor of order unity

$$f(z) = \frac{2}{\pi} \int_0^\infty (x+z) \cos^{-1} \left(\frac{z}{x+z} \right) \times \exp(-x) dz \quad (6)$$

In making bright-limb measurements, it is important to have a small slant distance to the planet limb in order to make $4\pi\mathcal{A}$ (off-axis) less than, or at most, of the same order as the intensities of the lines or bands to be measured.

Let us examine the geometry necessary to convert bright-limb intensity measurements into an altitude distribution for a given atmospheric constituent. In this discussion, the atmospheric constituent will be assumed to be optically thin in both the excitation process and the emitted radiation. This is true at higher altitudes where the number density of the constituent is small. When this is not the case, i.e., if the optical depth approaches $\tau = 1$ lower in the atmosphere, then the analysis is more complicated, but still straightforward.

In the optically thin case, the intensity is proportional to the number of atoms or molecules/cm² column, N (along the instrument axis) of the species leading to the emission, so that

$$4\pi\mathcal{A} = gN. \quad (7)$$

The constant, g , or emission rate factor, contains the atomic constants that describe the process and, in general, is proportional to the solar flux, πF , and the cross section, σ , for the process. In the case of more complicated processes such as photo-electron-excited dayglow, branching ratios are included in g (Barth, 1969). The observed lines must be optically thin in

order to infer altitude distribution, i.e., the optical depth, $\tau = \sigma N$, must be less than 1.

Let us relate the column density to the number density, $n(R)$, of an emitting constituent which obeys the barometric law

$$n(R) = n(R)_0 \exp[-(R - R_0)/H]. \quad (8)$$

The scale factor is H and R is measured from the center of the planet. The vertical column density for an isothermal atmosphere above R is

$$N_v(R) = n(R)H. \quad (9)$$

In Fig. 8, consider the evaluation of the column density, $N(R_0, \xi)$, along a ray originating at radius R_0 and making an angle ξ with the local zenith. The Chapman function defined as

$$\text{Ch}(\xi, R_0/H) \equiv \frac{N(R_0, \xi)}{N_v(R_0)} \quad (10)$$

was first investigated by Chapman (1931). The Chapman function has more recently been investigated by Swider (1964) and by Green and Martin (1966). A new analysis leads to a convenient expansion applicable to all values of the zenith angle, ξ . The Chapman function can be written as

$$\text{Ch}(\xi, R_0/H) = \frac{\int_{R_0}^\infty n(R) V(\xi, R_0/R) dR}{\int_{R_0}^\infty n(R) dR} \quad (11)$$

for $\xi \leq 90$ deg and where the kernel is the Van Rhijn function

$$V(\xi, R_0/R) = [1 - (\sin^2 \xi)(R_0/R)^2]^{-1/2}. \quad (12)$$

Subsequent analysis gives

$$\text{Ch}(\xi, x) = \lim_{\substack{\alpha \rightarrow 2 \\ \beta \rightarrow x}} \sum_{l=0}^L \frac{(-1)^l}{l!} \left(1 - \frac{\partial}{\partial \beta} \right) \times \frac{\partial^{2l} G(\alpha, \beta)}{\partial \alpha^l \partial \beta^l}. \quad (13)$$

The generating function is

$$G(\alpha, \beta) = \left(\frac{\pi}{\alpha\beta} \right)^{1/2} x \exp \left[(\cos^2 \xi) \left(\frac{\beta}{\alpha} \right) \right] \times \text{erfc} \left[(\cos^2 \xi) \left(\frac{\beta}{\alpha} \right) \right]^{1/2} \quad (14)$$

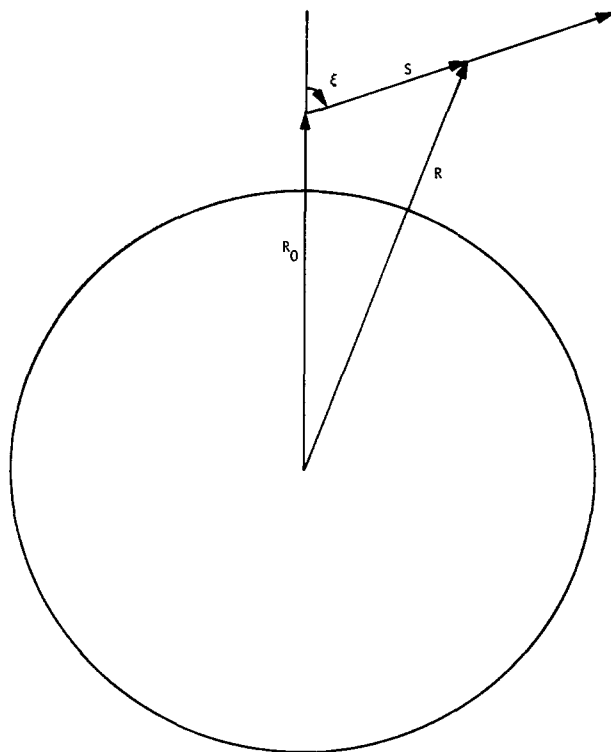


FIG. 8. Chapman function geometry.

where $\text{erfc}(x)$ is the complementary error function. The solution for the Chapman function can be written

$$\text{Ch}(\xi, x) = \text{Ch}^{(0)}(\xi, x) + \text{Ch}^{(1)}(\xi, x) + \dots \quad (15)$$

The first few terms of the expansion are

$$\begin{aligned} \text{Ch}^{(0)} &= (\pi x/2)^{1/2} \exp \rho \text{erfc} \rho^{1/2} \\ \text{Ch}^{(1)} &= -(1/x)[(\rho - \frac{1}{2}) \text{Ch}^{(0)} - \eta] \\ \text{Ch}^{(2)} &= -(1/2x)[(-\rho^2 - \rho + \frac{1}{4}) \text{Ch}^{(0)} \\ &\quad + (\rho + \frac{1}{2}) \eta] \\ \text{Ch}^{(3)} &= (1/2x^2)[(-\rho^3 - \frac{3}{2}\rho^2 + \frac{3}{4}\rho - \frac{3}{8}) \text{Ch}^{(0)} \\ &\quad + (\rho^2 + \rho - \frac{3}{4}) \eta], \end{aligned} \quad (16)$$

where

$$\rho = (x/2) \cos^2 \xi \quad (17)$$

and

$$\eta \equiv (x/2) \cos \xi. \quad (18)$$

Additional terms can be found from a recurrence relation. In practice, when

$x = R_0/H$ is large, as is usually the case, then

$$\text{Ch}(\xi, x) \approx \text{Ch}^{(0)}(\xi, x) + \text{order}(1/x). \quad (19)$$

When ξ is small, $\text{Ch}^{(0)}(\xi, x)$ reduces to $\sec \xi$ and when $\xi = 90^\circ$, it becomes the Hunten approximation (Hunten, 1954)

$$\text{Ch}^{(0)}(90^\circ, x) = \left(\frac{\pi H}{2 R_0}\right)^{1/2}. \quad (20)$$

The column density along the ultraviolet spectrometer optic axis from an orbiter above a planetary atmosphere is

$$N(R) = 2N_v(R) \text{Ch}(90^\circ, R/H) \quad (21)$$

or

$$N(R) = n(R)(2\pi RH)^{1/2}. \quad (22)$$

The ultraviolet spectrometer then essentially samples the atmosphere at a point along the optic axis that passes closest to the planet. Because of the weak dependence of the square-root factor, the

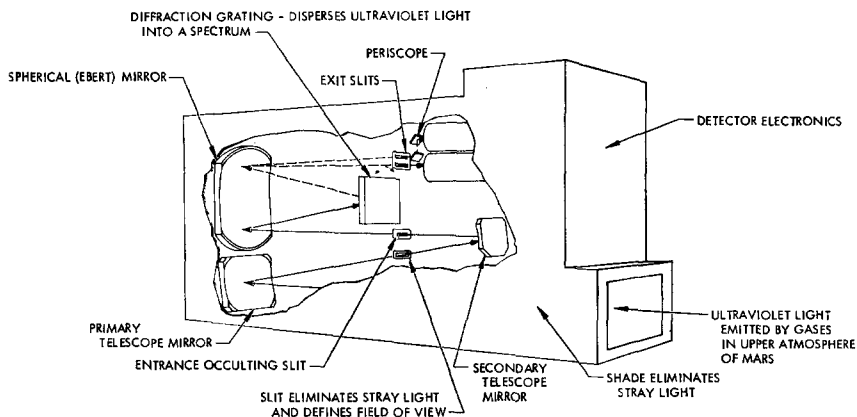


FIG. 9. Optical layout and physical configuration of ultraviolet spectrometer.

intensity is proportional to the number density at the sample altitude

$$4\pi\mathcal{A} = gn(R)(2\pi R_0/H)^{1/2}. \quad (23)$$

In cases where a constituent such as hydrogen is escaping, a more succinct representation can be made in terms of functions of the form

$$n(R) = n(R_0)(R_0/R)^k. \quad (24)$$

In this case, the intensity as a function of sample altitude number density, $n(R)$, can be found by substituting Eq. (24) into Eq. (11)

$$4\pi\mathcal{A} = gn(R)R \frac{2(\pi)^{1/2} \Gamma[\frac{1}{2}(k+1)]}{(k-1) \Gamma(\frac{1}{2}k)}. \quad (25)$$

Equations (23) and (25) are exact only when the solid angle of the instrument is infinitesimal. In the case of the Mariner ultraviolet spectrometer, the field of view of the F channel (1700 to 3400 Å) is 0.25 deg square and the G channel (1100 to 1700 Å) is 0.25 by 2.5 deg. For the G channel, the platform pointing angles can be chosen to align the projected spectrometer slit with the bright limb of Mars, providing an enhanced signal from small scale height species. For the anticipated orbits for the 1971 orbital mission, the slant distances to the bright limb of Mars will provide good altitude resolution. For exospheric hydrogen or when the scale height of the constituent is larger than the projected field of view of the instrument, the effect of the instrument's finite field of

view is negligible. When the projected field of view becomes comparable to the scale height, the intensity as seen by the instrument is

$$4\pi\mathcal{A} = g \left(\int N d\Omega / \int d\Omega \right). \quad (26)$$

If the slant distance is S and the half-cone angle of the rectangular field of view is θ , then it can be shown that the intensity is

$$4\pi\mathcal{A} = gN(R) \left[\frac{\sinh(\theta S/H)}{(\theta S/H)} + \text{order} \left(\frac{\theta S}{R} \right) \right], \quad (27)$$

where $N(R)$ is the column density along the spectrometer optic axis.

V. INSTRUMENT DESCRIPTION

The instrument to be used is an Ebert scanning spectrometer with an occulting slit telescope and a baffling system for the elimination of stray light. The optical layout and physical configuration of the instrument are shown in Fig. 9. The short-wavelength detector, 1100 to 1700 Å, is referred to as the G channel, while the longer wavelength detector, 1700 to 3400 Å, is referred to as the F channel. The G channel detector is a photomultiplier tube with a cesium iodide photocathode and a lithium fluoride window; the F channel detector uses a photomultiplier tube with a cesium telluride photocathode and a sapphire window. The characteristics that make these particular detectors desirable

are discussed by Barth (1969). The electronics are linear for both channels. The necessary dynamic range, to make low-intensity airglow measurements as well as high-intensity bright disk observations on the F channel, will be achieved by having feedback-controlled gain changes. The gain change will be accomplished by varying the high voltage applied to the F tube.

The Mariner ultraviolet spectrometer scans its range with a 3-sec period and gives a spectrum with 20-Å resolution. Wavelength scanning is accomplished by a grating movement driven by a cam. In addition to taking complete ultraviolet spectra, the design of the electronic subsystem allows for sampling at 1216 Å (Lyman- α) in order to utilize a lower data rate mode. This capability allows Lyman- α data to be taken for a larger percentage of each orbit.

VI. BIOLOGICAL INFERENCES

If biological activity is occurring, then one would expect that the atmosphere must betray its existence and be modified accordingly. The atmospheric algorithm for biological activity is only partially specified at this point in time. One of the important factors is that O₂ may exist only in trace abundances in the absence of biological activity (Urey, 1959; Berkner and Marshall, 1966). The presence of O₂ at a biologically significant threshold is detectable by an ultraviolet spectrometer because of the accompanying formation of O₃ (Barth, 1969). Many other chemically active components of the Earth's atmosphere, which may also be present in the Martian atmosphere, can be detected by ultraviolet spectroscopy. For example, OH, NO₂, NO, and CO can be detected in trace abundances. Other atmospheric gases, such as N₂, can be detected if they are major constituents. Hitchcock and Lovelock (1967) discuss how variations in the amounts of these constituents from thermodynamic equilibrium abundances may be indicative of life. Biological activity, if it is developing, may well send up its atmospheric smoke signal in advance of more overt physical signs of its existence.

REFERENCES

- ANDERSON, G. P., BARTH, C. A., CAYLA, F., AND LONDON, J. (1969). Satellite observations of the vertical ozone distribution in the upper stratosphere. *Ann. Geophys.* **25**, 341-345.
- BARTH, C. A. (1969). Planetary ultraviolet spectroscopy. *App. Optics* **8**, 1295-1304.
- BARTH, C. A., AND MACKEY, E. F. (1969). OGO-4 Ultraviolet Airglow Spectrometer. *IEEE Trans. on Geosci. Elec.* **7**, 114-119.
- BARTH, C. A., PEARCE, J. B., KELLY, K. K., WALLACE, L., AND FASTIE, W. G. (1967). Ultraviolet emissions observed near Venus from Mariner V. *Science* **158**, 1675-1678.
- BARTH, C. A., WALLACE, L., AND PEARCE, J. B. (1968). Mariner V measurement of Lyman- α radiation on Venus. *J. Geophys. Res.* **73**, 2541-2545.
- BELTON, M. J. S., AND HUNTEN, D. M. (1968). A search for O₂ on Mars and Venus: A possible detection in the atmosphere of Mars. *Astrophys. J.* **153**, 963-974.
- BERKNER, L. V., AND MARSHALL, L. C. (1966). Limitation on oxygen concentration in a primitive planetary atmosphere. *J. Atmos. Sci.* **23**, 133-143.
- CHAPMAN, S. (1931). The absorption and dissociative of ionizing effect on monochromatic radiation in an atmosphere on a rotating Earth. Part II, Grazing incidence. *Proc. Phys. Soc. London* **43**, 483-501.
- DALGARNO, A., McELROY, M. G., AND STEWART, A. I. (1969). Electron impact excitation of the dayglow. *J. Atmos. Sci.* **26**, 753-762.
- EVANS, D. C. (1965). Ultraviolet reflectivity of Mars. *Science* **149**, 969-972.
- GREEN, A. E. S., AND BARTH, C. A. (1967). Calculation of the photoelectron excitation of the dayglow. *J. Geophys. Res.* **72**, 3975-3986.
- GREEN, A. E. S., AND MARTIN, J. D. (1966). A generalized Chapman function. "The Middle Ultraviolet: Its Science and Technology" (A. E. S. Green, ed.) Wiley, New York.
- HITCHCOCK, D. R., AND LOVELOCK, J. E. (1967). Life detection by atmospheric analysis. *Icarus* **7**, 149-159.
- HUNTEN, D. M. (1954). A study of sodium twilight. I. Theory. *J. Atmos. Terr. Phys.* **5**, 44-56.
- KLIORE, A., CAIN, D. L., LEVY, G. S. (1967). Radio occultation measurement of the Martian atmosphere over two regions by the Mariner IV space probe. In "Moon and Planets," Proceedings of the 7th International Space Science Symposium of COSPAR. North-Holland Publ. Co., Amsterdam.
- POLLACK, J. B. (1967). Rayleigh scattering in an optically thin atmosphere and its application to Martian topography. *Icarus* **7**, 42-46.

- POLLACK, J. B., AND SAGAN, C. (1967). An analysis of Martian photometry and polarimetry. *Smithsonian Astrophys. Obs. Spec. Rept.* **258**; *Space Sci. Revs.* **9**, 243-299 (1969).
- REA, D. G., AND O'LEARY, B. T. (1965). Visible polarization data on Mars. *Nature* **206**, 1138-1140.
- SAGAN, C., AND POLLACK, J. B. (1966). Elevation differences on Mars. *Smithsonian Astrophys. Obs. Spec. Rept.* **221**. Also *J. Geophys. Res.* **73**, 1373-1387 (1968).
- SWIDER, W., JR. (1964). The determination of the optical depth at large solar zenith distances. *Planetary Space Sci.* **12**, 761-782.
- THOMAS, G. E. (1963). Lyman- α scattering in the Earth's hydrogen geocorona, I. *J. Geophys. Res.* **68**, 2639-2667.
- TOUSEY, R. (1963). The extreme ultraviolet spectrum of the Sun. *Space Sci. Rev.* **2**, 3-69.
- UREY, H. C. (1959). The atmospheres of the planets. *Handbuch der Physik* **52**, 363-418.